Proteomics Profiling of Human Synovial Fluid Suggests Increased Protein Interplay in Early-Osteoarthritis (OA) That Is Lost in Late-Stage OA

Authors

Neserin Ali, Aleksandra Turkiewicz, Velocity Hughes, Elin Folkesson, Jon Tjörnstand, Paul Neuman, Patrik Önnerfjord, and Martin Englund

Correspondence

neserin.ali@med.lu.se

In Brief

This study presents data of the proteome in *human* synovial fluid from three groups representing early-stage knee OA, end-stage knee OA, and controls without knee OA. The early stage had an increased protein activity, while in end-stage OA, there was a loss of interplay between the proteins. These results highlight the importance of studying the early stage of OA progression and that the interplay between the proteins may be an additional key element in disentangling the complex OA pathogenesis.

Graphical Abstract

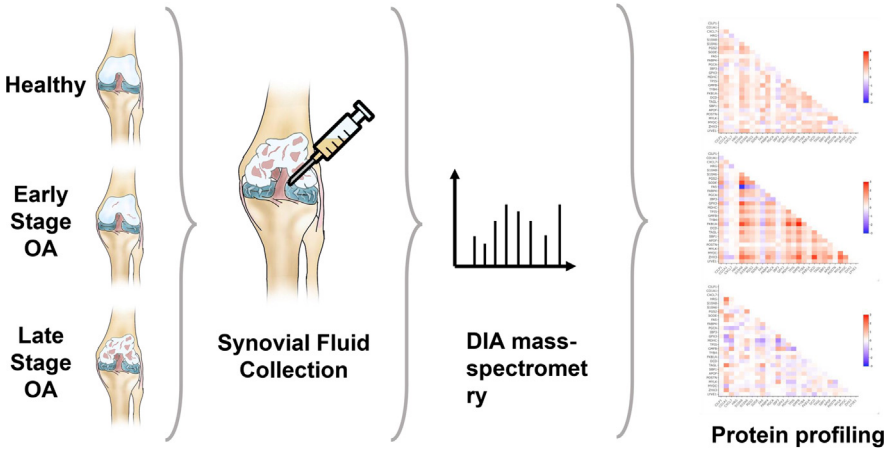

Highlights

- Synovial fluid proteomics study of different stages of osteoarthritis (OA).
- Higher catabolic activity is found in both early- and late-stage OA.
- Imbalance of the metabolic homeostasis in late-stage OA.
- Understanding early-stage OA may lead to finding better effective therapies.

2022, Mol Cell Proteomics *21*(*3*), 100200

https://doi.org/10.1016/j.mcpro.2022.100200

Proteomics Profiling of Human Synovial Fluid Suggests Increased Protein Interplay in Early-Osteoarthritis (OA) That Is Lost in Late-Stage OA

Neserin Ali[1,*], Aleksandra Turkiewicz[1], Velocity Hughes[1], Elin Folkesson[1,2], Jon Tjörnstand[3], Paul Neuman[3], Patrik Önnerfjord[2,‡], and Martin Englund[1,‡]

The underlying molecular mechanisms in osteoarthritis (OA) development are largely unknown. This study explores the proteome and the pairwise interplay of proteins in synovial fluid from patients with late-stage knee OA (arthroplasty), early knee OA (arthroscopy due to degenerative meniscal tear), and from deceased controls without knee OA. Synovial fluid samples were analyzed using state-of-the-art mass spectrometry with data-independent acquisition. The differential expression of the proteins detected was clustered and evaluated with data mining strategies and a multilevel model. Group-specific slopes of associations were estimated between expressions of each pair of identified proteins to assess the co-expression (*i.e.*, interplay) between the proteins in each group. More proteins were increased in early-OA *versus* controls than late-stage OA *versus* controls. For most of these proteins, the fold changes between late-stage OA *versus* controls and early-stage OA *versus* controls were remarkably similar suggesting potential involvement in the OA process. Further, for the first time, this study illustrated distinct patterns in protein co-expression suggesting that the interplay between the protein machinery is increased in early-OA and lost in late-stage OA. Further efforts should focus on earlier stages of the disease than previously considered.

Osteoarthritis (OA), a degenerative joint disease, is one of the most common chronic health conditions and a leading cause of pain and disability among adults (1, 2). Signs of OA are present in five percent of the population between the age of 35 to 54 years, and the occurrence of the disease increases with age (3, 4). OA is a disease that can affect the whole joint; the hallmark of the disease is destruction of the articular cartilage and alterations of the subchondral bone, characteristic changes of the meniscus, cruciate ligament, and synovial thickening (5, 6). Despite the high burden of OA, its pathogenesis remains unclear (2, 7). The mechanisms involved in disease progression include mechanical, inflammatory, and metabolic system failure, causing alterations of the different compartments of the joint (5, 6, 8–12). Therapeutic strategies are targeted at reducing mechanical malalignment, inflammation, and pain, and no pharmacological treatment has been able to reverse OA progression in the long term (13).

The classic diagnosis of OA relies on the presence of clinical symptoms in combination with radiographic findings of joint degeneration, which are seen at a relatively late stage of the disease (14). Thus, the search for reliable biomarkers to diagnose OA and to assess its risk of progression is at the utmost importance (15). Discovery of OA biomarkers would be useful in identifying individuals with early disease, *e.g.*, for recruitment to clinical trials, as well as for supplementary monitoring of effects of therapies aimed at disease modification. Finding good biomarkers representing the progression of OA goes hand in hand with exploring the pathogenesis. Former studies to disentangle the molecular pathogenesis of OA or to identify biomarkers have typically focused on specific molecules or signaling pathways (15–17). However, the "single biomarker strategy" has over and over again shown its lack of sensitivity and specificity for progression of the disease (17–19). In contrast, the cross talk between molecules could be very informative to explore and gain deeper insights into the molecular pathogenesis of OA (20, 21).

While a number of different omics studies have been carried out (22–28), they were limited by the technologies used or availability of biological samples. The difficulties in obtaining synovial fluid from individuals with no OA or other joint diseases has limited the ability to associate measured molecular changes to disease progression (22, 24). However, discovery-based approaches have been improved so a deeper molecular

From the [1]Clinical Epidemiology Unit, Division of Orthopedics, and [2]Division of Molecular Skeletal Biology, Section for Rheumatology, Department of Clinical Sciences Lund, Lund University, Lund, Sweden; [3]Department of Orthopedics, Skåne University Hospital, Lund, Sweden

‡Shared senior authors.

*For correspondence: Neserin Ali, neserin.ali@med.lu.se.

https://doi.org/10.1016/j.mcpro.2022.100200

coverage can be obtained, with the ability to quantify a higher number of proteins in comparison to what has previously been done (26). Therefore, the aim of this study is to explore disease stages of OA using a discovery approach based on state-of-the-art mass spectrometry (MS) instrumentation and methodology. The disease stages were represented by human synovial fluid from (1) patients with late-stage knee OA, (2) patients with degenerative meniscal tears (indicative of early-stage OA), and (3) controls without OA, to explore the differential expression and the pairwise interplay of proteins measured.

EXPERIMENTAL PROCEDURES

Materials

The micro bicinchoninic acid protein assay kit and Nanosep 30K Omega Centrifugal Devices were purchased from Pall Life Sciences, and SOLAμ Solid Phase Extraction HRP 2 mg/1 ml 96-well plates were purchased from Thermo Fisher Scientific. Trypsin (sequencing grade) was purchased from Promega Corporation. Calcium chloride, formic acid (FA), hydrochloric acid, and ammonium acetate were purchased from Merck. DTT and iodoacetamide were purchased from Sigma-Aldrich. Acetonitrile (ACN) was purchased from Sigma-Aldrich.

Experimental Design and Statistical Rationale

Synovial fluid was sampled from three different types of subjects from the MENIX biobank at Skåne University Hospital, Lund: (i) end-stage medial compartment knee OA patients undergoing total knee arthroplasty (n = 11 [three men and eight women], age range 55–80 years), the arthroplasty synovial fluid selected for this study will hereafter be called late-stage OA synovial; (ii) knee arthroscopy patients who had a typical degenerative meniscal tear (n = 7 [three men and four women], age range 50–64 years), the arthroscopy synovial fluid selected for this study will hereafter be called early-stage OA synovial; and (iii) human deceased donors (controls), without evidence of tibiofemoral OA or known clinical knee OA (n = 13 [five men and eight women] age range 19–79 years). All human deceased donor samples were obtained within 48 h postmortem, and the specimens were frozen at –80 °C within 2 h of extraction. To be eligible as controls, the donor menisci were required to be macroscopically intact. Further, the femoral cartilage (the load bearing region) from the medial compartment of the same donors (also in the biobank) were inspected and required the cartilage to be macroscopically intact. The synovial fluid samples were obtained by transcutaneous aspiration immediately prior to the respective procedures. The donor synovial fluid selected for this study will hereafter be called control synovial. All synovial fluids were centrifuged at 1800 rpm for 10 min, and supernatants and pellets were separately frozen and stored at –80 °C. The synovial fluid samples' selection criteria from the biobank were also based on no visual signs of blood contamination. Informed consent was taken before collecting the samples for biobanking. The sample collection and analysis has been proven by the ethical review committee of Lund University (Durs: 2015/39;2016/865; 2019/3239) and carried out in accordance with relevant guidelines and regulations by the Declaration of Helsinki principles.

Sample Preparation

The total protein content in the synovial fluid sample was determined using a bicinchoninic acid protein assay kit and carried out after each sample preparation step to make sure that the samples were equally effected. From each sample, 50 μl synovial fluid was mixed with 10 μl MS-safe proteinase inhibitor cocktail, 10 μl hyaluronidase, and 10 μl/μg protein and further incubated for 3 h at 37 °C. Four out of the seven samples in the early OA samples were diluted with saline solution during sampling of synovial fluid; these samples were adjusted to the mean total protein content calculated from the remaining three samples in that group. All samples were depleted of the seven most abundant proteins with the multiple affinity removal system (MARS Hu7 spin cartridge) according to the manufacturers protocol (Agilent Technologies). Samples were further reduced using 4 mM DTT, while shaking at +56 °C for 30 min and alkylated using 16 mM iodoacetamide for 1 h at room temperature in the dark. To remove residual salts, the samples were precipitated with 1:9 volume 95% ethanol alcohol (with 50 mM sodium acetate) at 4 °C overnight. The precipitated samples were centrifuged at 13,000 rpm for 1 h, and the supernatants were removed from the pellets. The samples were dissolved in 0.1 M ammonium bicarbonate and digested with sequencing grade trypsin (Promega) at a protease/protein ratio of 1:50, overnight at 37 °C. Following digestion, samples were cleaned up with a 30 kDa filter (Pall Life Sciences), and the flow-through was desalted with C18 96-well plates (SOLAμ Thermo Fisher Scientific). The samples were further spiked with iRT peptides before analyses with MS.

Instrumentation and Data Analysis

The samples were analyzed with an EASY-nLC 1000 (Thermo Scientific) coupled to a Thermo Scientific Q-Exactive HFX mass spectrometer using data-independent acquisition (DIA). For liquid chromatography, mobile phase A consisted of water containing 0.1% FA and mobile phase B consisted of ACN containing 0.1% FA. Peptides were loaded on an Acclaim PepMap 100 nanoViper pre-column (Thermo Scientific, C18, 3 μm particles, 75 μm i.d. 2 cm long) at 5 μl/min mobile phase A. The peptides were separated on a PepMap RSLC C18 analytical column (Thermo Scientific, C18, 2 μm particles, 75 μm i.d. 25 cm long) at 300 nl/min using an ACN/FA gradient consisting of an initial step of 5 to 7% B over 5 min followed by 7 to 20% B over 85 min, 20 to 30% B over 20 min, 30 to 90% B over 5 min, held at 90% B for 5 min, and then equilibrated for 15 min at 3% B. Separation was performed at 45 °C, and the total acquisition time was 125 min. DIA settings: method duration 125 min, full scan resolution 120,000, and scan range 350 to 1650 m/z. Automatic gain control (AGC) target 3.0e6, maximum injection time 100 ms, Orbitrap resolution 45,000, AGC 3.0e5 with a variable isolation window 33/26/22/20 × 2/18/20/19 × 4/20/21 × 2/23 × 2/24/26/31/32/37/40/53/66/99/574 m/z, and normalized collision energy 27 eV. Data-dependent acquisition settings: method duration 125 min, mass range 350 to 1650 m/z., full MS scan resolution 120,000, AGC 3e6, maximum injection time 20 ms, Orbitrap resolution 15,000, AGC target 1.0e5, maximum injection 20 ms, normalized collision energy 27 eV. The MS raw data were further analyzed with SpectronautPulsar software (version 12.0.20491.15, Biognosys AG) for protein identification and quantitative data extraction. In total, 118 runs were used from both the data-dependent acquisition, and DIA files were converted to HTRMS format using HTRMS Converter (Biognosys AG) to generate the spectral library. The human protein fasta files were downloaded from the UniProt database (20190416). Default settings were used with additional modifications: cysteine carbamidomethylation was used as a fixed modification, and deamination, pyro-glutamic acid (N-term Glu to pyroglutamic acid), methionine oxidation, hydroxyproline, and acetylation were used as variable modifications. Using trypsin/P as the specific digestion type with maximum of two miss cleavages. A subsequent protein search was conducted in Spectronaut Pulsar using the recently created spectral library and the same human database as

background proteome. Precursor quantitation was performed at MS2 level, and the area under the curve was used for quantitation (supplemental Table S1).

Statistical Analysis

The quantitative data were extracted using SpectronautPulsar software. The differential expression of proteins between the different groups was analyzed using a linear mixed effects model with the sample group, protein type, and their interaction as independent variables and subject as a random effect to account for clustering of proteins within an individual and transformed differential expression as the outcome (29).The protein expression was transformed using logarithm with base two before the analysis. Further, the model was adjusted for age, sex, and body mass index. Only proteins that had a maximum of one missing value in the early-stage OA group, two missing values in the late-stage OA group, and two missing values in the control group were included to enable enough samples for estimation which includes 406 proteins. Residual diagnostics confirmed adequate model fit. As the sample size of the early-stage OA group was lower than the others due to sample unavailability and also because this group had the highest amount of missing data on protein differential expression, a sensitivity analysis was performed where the early-stage OA group was removed, allowing a larger set of proteins to be included in this analysis, 474 proteins (compared to 406 proteins when including all three groups). Proteins were considered differentially expressed when the 95% confidence interval of the log2 fold change did not include zero.

Data Visualization and Presentation

Clustering—Principal component analysis (PCA) was used to cluster the samples based on their protein expression data. After filtering out proteins based on missing values (max one missing value for the early-stage OA group and two for the control and late-stage OA groups, as described above), 406 proteins were included in the analysis. The rest of the missing values were substituted with 0. PCA preprocessing included a Pareto scaling using "RFmarkerDetector::paretoscale" functions in R.

Protein–Protein Co-Expression—The linear associations between pairs of proteins expression and estimates of the regression slopes for each group were conducted. This by fitting a linear regression model for each pair of proteins (82,418 models in total) with expression of one of the proteins as outcome and expression of the other protein, the group, and their interaction as independent variables. The intensities were transformed with logarithm of base two before fitting the models and standardized by subtracting mean protein expression and dividing by the standard deviation, to make the slopes comparable between models.

Pathway Analysis

To evaluate common interactions and pathways of the identified proteins with changed levels, the results were further analyzed with IPA software (Ingenuity Systems, www.ingenuity.com). Differentially expressed proteins were mapped and compared to known pathways, diseases, functions, and connecting regulators using only 406 proteins as a background dataset. The data were also evaluated based on canonical pathways and upstream regulators with positive z-scores (activating capacity) and negative z-scores (inhibiting capacity). Only enriched canonical pathways and upstream regulators with an absolute z-score ≥ 2 were further discussed. Key regulators are proteins with an earlier established association with the activation or inhibition of many of the identified proteins, but the regulators not necessarily detected themselves in our MS analysis. Default settings were used except for species, which was set to human. In addition, only experimentally observed relationships were considered. The software was unable to map P69905 protein (hemoglobin subunit alpha). This protein was therefore not further included in the pathway analysis.

Reproducibility and Quality Control

The samples were run in random order with the insistency of having samples from each group analyzed in the beginning, middle, and the end of the sample batch run. A pooled sample was run every 10th sample as a quality control sample. Eighteen of the samples were run as duplicates to check for reproducibility. The reliability was evaluated by comparing two injections of the same sample and estimating the agreement using the Bland–Altman method (30, 31). The data were again transformed by the logarithm of base two to stabilize variance.

Validation of Mass Spectrometry Results

Thirty-six out of the 406 proteins that were differentially expressed in our MS data were further validated with the Multiplex cardiometabolic immunoassay panel (Olink Proteomics), and the panel was chosen based on the highest number of proteins also detected with the discovery-based MS technique. The synovial fluid samples were diluted 1:1000 before analysis. Processing, output data quality check, and normalization were performed by Olink Proteomics. All data were delivered as normalized protein expression values on a $\log_2$ scale. Data values below the level of detection were removed from the dataset. Using these data, the main analysis was repeated with linear multilevel models to estimate the differences between the groups in protein expression and relate them to the original results.

RESULTS

Label-Free Quantification

In total, 715 proteins were detected and relatively quantified in synovial fluid samples from 31 subjects. After selection of proteins with limited missing values, 474 proteins were eligible for the clustering and statistical analysis for comparing the late-stage OA *versus* control group and 406 proteins for comparing all three groups.

Clustering

PCA revealed an unsupervised difference between the individual samples, clustering the samples very well in their different groups (Fig. 1*A*). The protein profile of early-stage OA synovial fluid samples clustered between control and late-stage OA samples. The biplot shows some of the proteins that drive this cluster separation (Fig. 1*B*). Among these are chemokine (C-X-C motif) ligand 7 (CXCL7), decorin (PGS2), S10A8, zinc fingers, and homeoboxes protein 3 (ZHX3).

Differentially Expressed Proteins

Out of 406 proteins analyzed, different patterns of protein expression were identified with over than 200 proteins that where differently expressed between the different groups (supplemental Fig. S1 and supplemental Table S2). Among them, 27 proteins (whereof 16 downregulated) with a fold change of 2 or larger in the late-stage OA group compared to control or in the early-stage OA group compared to control were identified (Fig. 2). The most pronounced differences in comparisons with controls were found for PGS2 (fold change

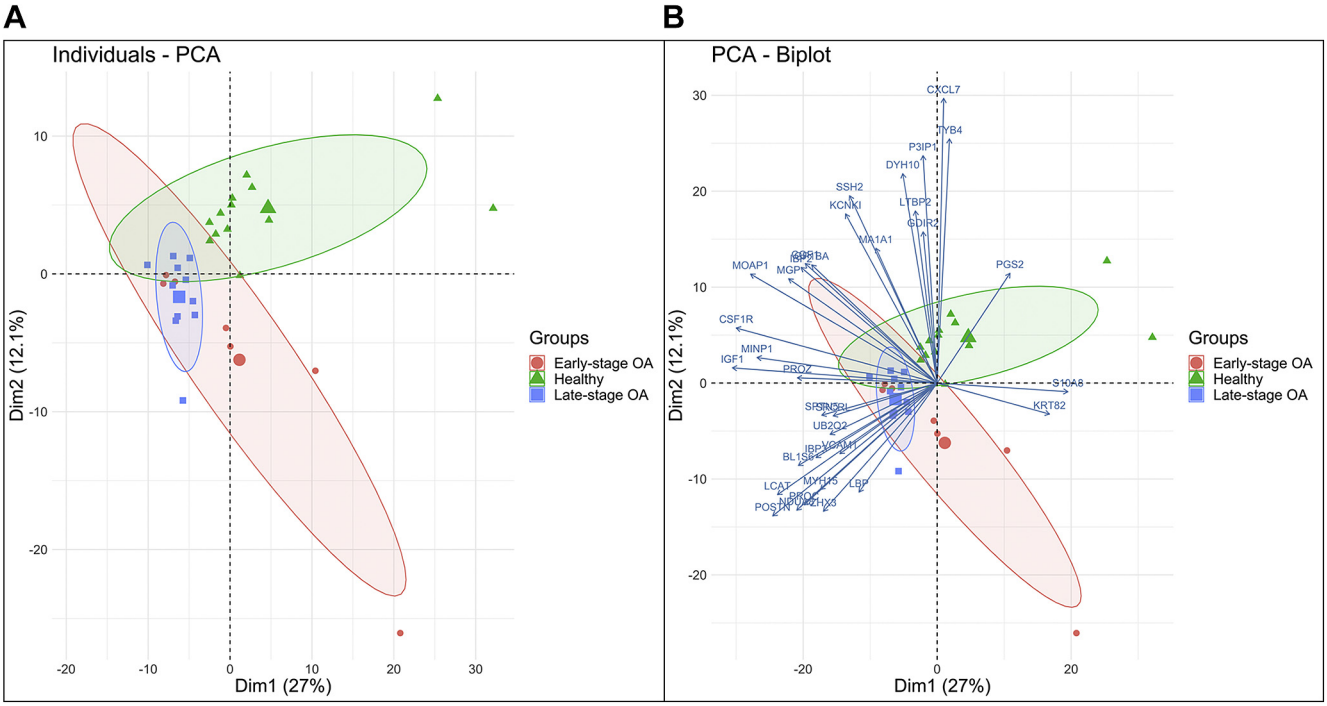

FIG. 1. **PCA and Biplot.** 406 proteins from the label free quantification were used to cluster the different samples. *A*, principal component analysis of each sample in each group driven by the label free quantification of the 406 proteins. *B*, biplot showing the proteins that drive the separation of the clusters. PCA, principal component analysis.

0.05 with a 95% CI [0.03–0.09] early-stage OA, 0.03 [0.02–0.06] late-stage OA), CXCL7 (0.091 [0.05–0.17] early-stage OA, 0.061 [0.03–0.11] late-stage OA). glutathione peroxidase 3 (8.85 [4.95–15.8] early-stage OA, 5.91 [3.29–10.63] late-stage OA) and histidine-rich glycoprotein (7.03[3.95–12.51] early-stage OA, 7.79 [4.35–13.95] late-stage OA), where >1-fold changes indicate higher levels in early-stage OA patients than in controls and vice versa. Inspecting the gradient from the lowest to the highest fold changes in differently expressed proteins (supplemental Fig. S1*A*), the majority of the proteins that differed between the late-stage OA and control cases were higher in the control samples in comparison to the late-stage OA samples. This observation was even more evident when only comparing the late-stage OA and control samples. When comparing late-stage OA and early-stage OA samples, only three proteins were higher in late-stage OA in comparison to early-stage OA—fibronectin, 1.99 [1.04–3.83]; hemoglobin subunit alpha, 2.25 [1.17–4.32]; and cartilage acidic protein 1 (CRAC1), 1.96 [1.02–3.78]—whereas 112 proteins were higher in early-stage OA than in late-stage OA samples (supplemental Fig. S1*B*). Together, all these results suggest an overall decrease in protein expression in late-stage OA.

Biological Relevance

Canonical Pathways—Pathway analysis revealed that the differentially expressed proteins were connected to multiple canonical pathways (Table 1). The z-scores suggest whether the pathways are activated or inhibited in accordance to the fold changes of the connected proteins. The pathway analysis predicted a strong activation of the liver X receptor–retinoid X receptor lipid metabolism pathway in early-stage OA (z-score 2.3) and late-stage OA groups (z-score 1.3) (Table 1).

Upstream Regulators—Pathway analysis also predicted that the differentially expressed proteins were connected to multiple upstream regulators (Fig. 3). For instance, the transcription factor peroxisome proliferator–activated receptor gamma (PPARG) was inhibited in the early-stage OA group in comparison to controls. The analysis also suggested that the peptide hormone resistin (RETN) is inhibited in the late-stage OA group in comparison to controls.

Molecular Functions—Pathway analysis revealed that the differentially expressed proteins were connected to multiple diseases and molecular functions (supplemental Fig. S2 and supplemental Table S3). The z-scores suggest whether the corresponding functions are activated or inhibited in accordance to the fold changes of the connected proteins. The overall pattern suggested that several molecular functions such as cellular development and assembly are activated in the early-stage OA group. It also suggested that cellular movement is deactivated in the late-stage OA group.

Inflammation—Pathway analysis suggests that the acute phase response pathway is inhibited in the early-stage OA (z-score –1.1) in comparison to the controls (Table 1). Leukocyte

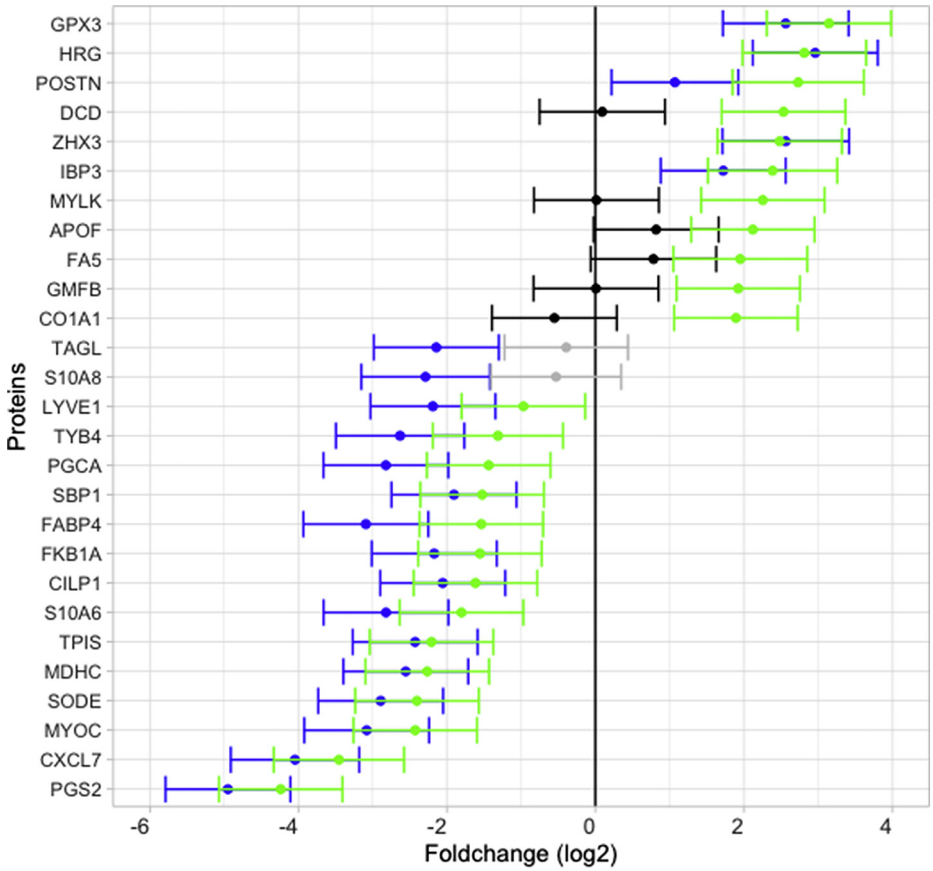

FIG. 2. **Differentially expressed proteins with an estimated fold change larger than 2.** Comparison between early-stage OA *versus* controls (*green* and *gray bars*), comparison between late-stage OA *versus* controls (*blue* and *black bars*). *Blue* and *green bars* represent differentially expressed proteins whose 95% CIs exclude 0. OA, osteoarthritis.

extravasation signaling is suggested to be activated in the early-stage OA group (z-score 1.0) compared to controls. Additionally, typical markers for inflammation (*e.g.*, CXCL17) were found to be decreased in the early-stage OA and late-stage OA cases in comparison to the controls (supplemental Table S2). The upstream regulatory analysis suggests an activated interleukin (IL)17 (z-score 2.0) in early OA but an inhibited CXCL12 (z-score −2.2) in late stage (Fig. 3).

Extracellular Matrix Organization and Damage-Associated Molecular Patterns—The results revealed multiple extracellular matrix (ECM) proteins that were differentially expressed in the synovial fluid when comparing the different groups to each other (supplemental Fig. S1 and supplemental Table S2).

Further several collagens were found to be differentially expressed, some of which are increased and other decreased between the different groups. CO18A1 (fold change 0.60 and 95% CI [0.34–1.07] early-stage OA, 0.38 [0.21–0.68] late-stage OA) and CO6A2 (0.47 [0.26–0.85] early-stage OA, 0.53 [0.30–0.96] late-stage OA) had a lower expression in both early-stage OA and late-stage OA cases in comparison to the controls, while CO5A1 (3.36 [1.89–5.98] early-stage OA, 2.25 [1.26–4.03] late-stage OA) had a higher expression in both early-stage OA and late-stage OA cases. CO3A1 (0.22 [0.11–0.42]), CO14A1 (0.34 [0.17–0.68]), and CO1A1 (0.18 [0.10–0.35]) all had a lower differential expression in the late-stage OA cases compared to early-stage OA cases. Some damage-associated molecular pattern proteins were also differentially expressed between the different groups, and fibrinogens (gamma, beta, and alpha) were lower in OA patients in comparison to controls. Tenascin (2.12 [1.19–3.77] early-stage OA, 2.13 [1.19–3.82] late-stage OA) was higher in OA patients in comparison to controls.

Serine Protease Activity—Differentially expressed proteins that were higher in OA patients in comparison to controls had serine-type peptidase activity; among them were MMP2 (fold change 1.91 and 95% CI [1.07–3.40] early-stage OA, 1.79 [1.00–3.20] late-stage OA) and MMP3 (2.38 [1.33–4.24] early-stage OA, 2.08 [1.16–3.72] late-stage OA).

Associations Between Pairs of Proteins

Protein co-expression analysis revealed that the control samples have protein pairs that are both positively and negatively co-expressed (mean slope, 0.29), whereas the early-stage OA co-expression revealed an increase in positive

TABLE 1
Pathway enrichment analysis

Comparison	Ingenuity canonical pathways	z-Score	Molecules
Early OA *versus* control	**LXR/RXR activation**	**2,3**	**AGT,AHSG,ALB,APOB,APOC1,APOF,APOM,C4A/C4B, FGA,KNG1,LBP,ORM1,PON1,SERPINF2,TTR**
	Neuroprotective role of THOP1 in Alzheimer's disease	**2,2**	**AGT,C1R,F11,HGFAC,HTRA1,KNG1,MASP1,YWHAE**
	Production of nitric oxide and reactive oxygen species in macrophages	**2,1**	**ALB,APOB,APOC1,APOF,APOM,CAT,ORM1,PON1**
	Unfolded protein response	**2**	**HSPA2,HSPA5,HSPA8,PDIA6**
	Hepatic fibrosis signaling pathway	1,6	AGT,COL1A1,COL3A1,ITGB1,MYLK,SPP1
	Phagosome formation	1,6	CFL1,ITGB1,LBP,MRC2,MYLK,TLN1
	Tumor microenvironment pathway	1,6	COL1A1,COL3A1,IGF1,MMP2,MMP3,SPP1,TNC
	Intrinsic prothrombin activation pathway	1,4	COL1A1,COL3A1,F10,F11,F13 B,F2,F5,F9,FGA,FGB, FGG,KLKB1,KNG1,PROC,PROS1
	MSP-RON signaling in cancer cells pathway	1,3	F11,HGFAC,ITGB1,KLKB1,YWHAE
	Estrogen receptor signaling	1,3	AGT,CFL1,IGF1,MMP2,MMP3,NDUFA8
	Leukocyte extravasation signaling	1	CDH5,ITGB1,MMP2,MMP3
	Synaptogenesis signaling pathway	1	CDH5,CFL1,HSPA8,TLN1
	HOTAIR regulatory pathway	1	COL1A1,COL3A1,MMP2,MMP3,SPP1
	Integrin signaling	1	ITGB1,MYLK,PFN1,TLN1
	BAG2 signaling pathway	1	CTSB,HSPA2,HSPA5,HSPA8
	Glycolysis I	−1	ALDOC,ENO1,GAPDH,TPI1
	RHOGDI signaling	−1	ARHGDIB,CDH5,CFL1,ITGB1
	SPINK1 pancreatic cancer pathway	−1	CPN1,CPQ,CTSB,KLKB1
	eNOS signaling	−1	HSPA2,HSPA5,HSPA8,KNG1
	Acute phase response signaling	−1,1	AGT,AHSG,ALB,C1R,C4A/C4B,F2,FGA,FGB,FGG,HRG, ITIH2,KLKB1,LBP,ORM1,SERPIND1,SERPINF2,TTR
Late OA *versus* control	LXR/RXR activation	1,3	AHSG,APOA4,APOB,FGA,KNG1,LBP,ORM1,PLTP, PON1,S100A8
	HIPPO signaling	1	CD44,YWHAE,YWHAG,YWHAZ
	Intrinsic prothrombin activation pathway	−1	COL18A1,COL3A1,F11,F9,FGA,FGB,FGG,KLKB1, KNG1,PROS1
	GP6 signaling pathway	−1,9	COL18A1,COL3A1,COL5A1,COL6A2,FGA,FGB,FGG
	Hepatic fibrosis signaling pathway	**−2,2**	**CCN2,COL18A1,COL3A1,FTH1,SPP1**

Differentially expressed proteins mapped to canonical pathways. The z-score is the probability score of activation if positive and deactivation if negative, only pathways with an absolute value of 1≥ are presented. Pathways with a z-score ≥2 was defined as the threshold of significant activation, whilst z-score ≤−2 was defined as the threshold of significant inhibition. The bold values indicate the canonical pathways with an absolute z-score that are equal to or larger than 2.

co-expression of the same protein pairs (mean slope, 0.48) (Fig. 4). The same analysis with late-stage OA samples indicated that co-expression between the proteins in these pairs was largely lost at this stage of the disease (mean slope, 0.05). The same pattern could be detected when comparing protein co-expression in all 406 proteins or when only selecting the differentially expressed proteins in one of the group comparisons but not the other, or even in proteins that did not show differential expression between any of the different groups (supplemental Figs. S3–S5).

Data Quality

In order to assess the reproducibility of our dataset, we have rerun randomly selected 18 samples from the cohort. Repeatability coefficients estimated using the Bland–Altman approach for the 406 proteins included in the main analysis (*i.e.*, the size of the difference between two measurements of the same sample) had (on a $\log_2$ scale) a median of 0.46, which corresponds to a fold change of 1.37. Seventy-five percent of the proteins had a repeatability coefficient lower than 0.83 (corresponding to a fold change of 1.77) (supplemental Results).

Validation of Mass Spectrometry Label-Free Quantification with Olink

A similar fold change pattern for 36 proteins was found as in the label-free MS results when they were validated using the immuno-based proximity extension assay from Olink (Fig. 5). Overall, the Olink data resulted in slightly higher fold changes than MS data. Olink data also had an overall lower dynamic range in comparison to the MS data.

DISCUSSION

The results of this study generated evidence of a profound difference in the protein profile of knee synovial fluid from controls compared to knee OA patients with more than 200

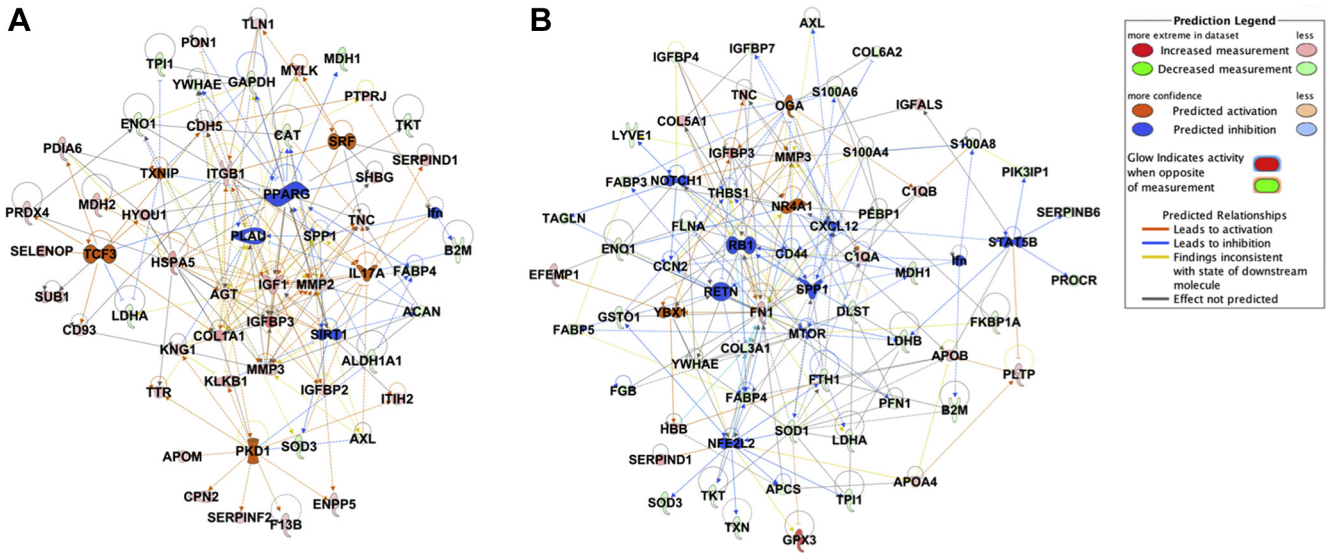

FIG. 3. **The network of upstream regulators.** *A*, upstream regulators suggested to be activated or deactivated by the differentially expressed proteins in the early-stage OA group. *B*, upstream regulators suggested to be activated or deactivated from the differentially expressed proteins in the late-stage OA group. OA, osteoarthritis.

proteins differentially expressed between the different groups. The overall view of the changed proteins can be associated with an increased catabolic activity on the extracellular matrix originating from the surrounding joint tissue, imbalance in the metabolic homeostasis, and a potential dysregulated effect on the synovial fluid clearance. The observed protein fold change patterns indicated an overall higher protein expression in early-stage OA and a reduced response in late-stage OA. Additionally, evaluation of the co-expression patterns of proteins within each of the three groups indicated that positive co-expression between proteins was increased in early-stage OA compared to controls, and that this co-expression was mostly lost in late-stage OA.

The data were analyzed both with an unsupervised dimensionality reduction test and PCA and through linear multilevel model (32–34). A lot of the proteins that were differentially expressed in the statistical model were also among the principal components separating the different samples from each other, resulting in separated clusters in-between the different groups.

Among the 27 proteins that were differentially expressed with a fold change larger than 2 have previously been reported to have a connection to OA disease progression (Fig. 4) (22, 35–40). Proteins like cartilage intermediate layer protein 1 (CILP), aggrecan core protein (ACAN, PGCA), decorin (DCN, PGS2), and collagen type I (COL1A1) have been identified in multiple studies to be associated with OA (41–43). CILP can act as an antagonist to transforming growth factor-β1-mediated induction of cartilage matrix genes and insulin-like growth factor 1-induced proliferation (44). Its overexpression may lead to impaired chondrocyte growth and matrix repair. It has previously been found to be increased in both early and late OA cartilage (45, 46). In this study, CILP was found to be decreased in both early-stage and late-stage OA synovial fluid. This may suggest an increase in ECM remodeling. The proteoglycan aggrecan (ACAN or PGCA) is a major component of the ECM of cartilaginous tissues (47). The major function of this protein is to resist compression in cartilage (48). It binds avidly to hyaluronic acid and forms negatively charged proteoglycan aggregates that attract water (49, 50). Cartilage aggrecan fragments have previously been detected in normal synovial fluid indicating a normal aggrecanase activity in response to catabolic turnover and with more fragmented aggrecan in late-stage OA (51). In our study, aggrecan was decreased in both early- and late-stage OA, which goes in line with previous study of increased fragmentation of aggrecan and increased catabolic activity (51). Decorin (DCN) belongs to the SLRP family. It binds to the surface of the completed fibril thereby providing for interactions with other components of the matrix. It can affect the rate of collagen type I fibril formation, influencing the crosslinking of the ECM (52). Decorin has previously been detected in synovial fluid of OA patients (22), and neopeptides have been shown to be present in synovial fluid of OA horses (40), which may be indications of increased proteolytic activity. These proteins also exist in normal articular cartilage and are present in the matrix surrounding chondrocytes (5, 53). In this study, all these three proteins were decreased in the synovial fluid of both early- and late-stage OA in comparison to the controls, which may be due to higher catabolic activity due to the disease. Periostin (POSTN) is associated with reparative processes involving cell adhesion and migration (54). It enhances incorporation of BMP1 in the fibronectin matrix of connective

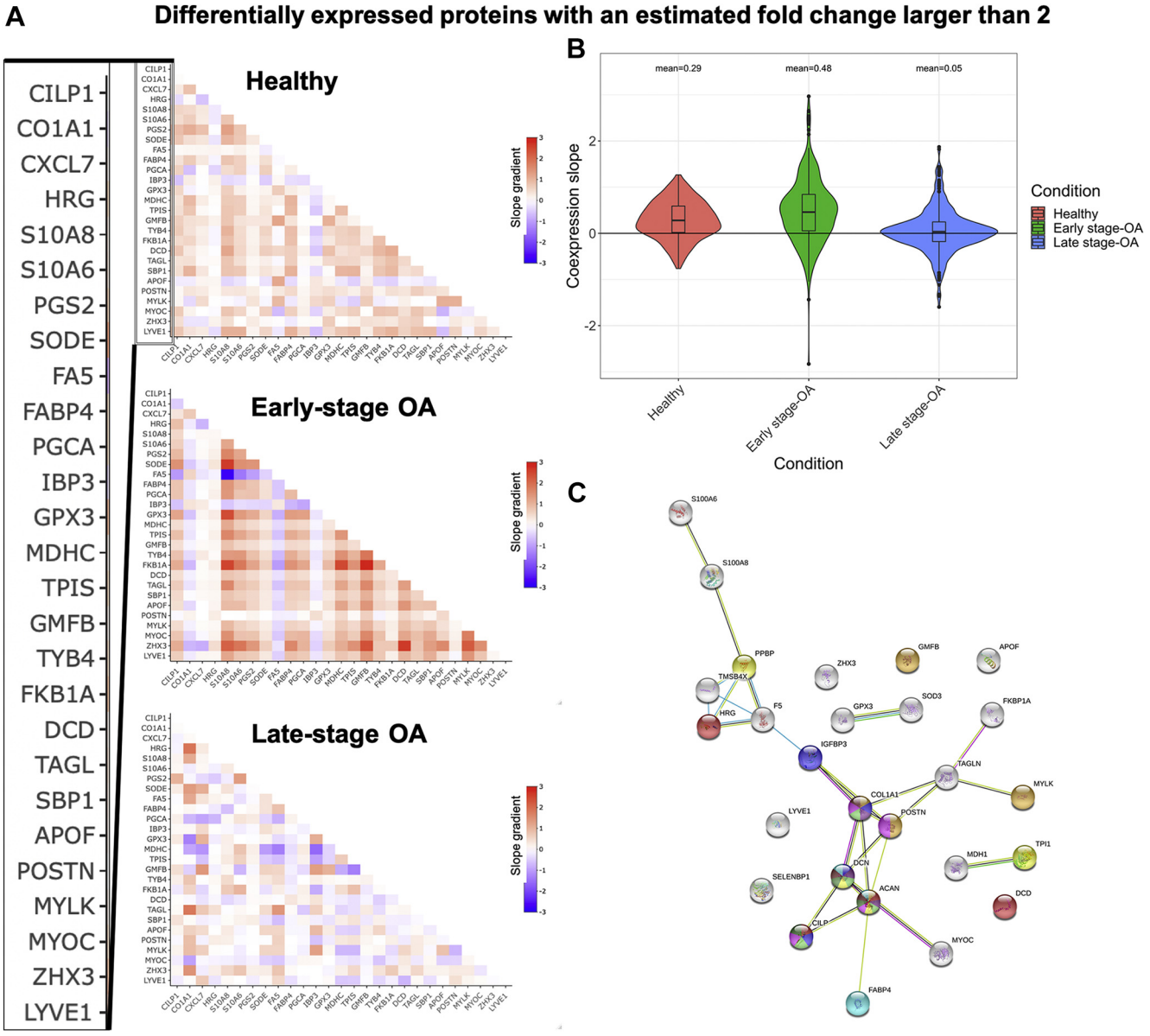

FIG. 4. **The estimated slope for each protein–protein co-expression pair between the 27 differentially expressed proteins with an estimated fold change larger than 2.** *A*, the estimated slopes for each protein–protein co-expression pair of the 27 differentially expressed proteins with an estimated fold change larger than 2 are represented on the x and y axes for a for each group. *B*, the distribution of the estimated slopes for each of the protein–protein co-expression, and the mean slope value is represented in the violin plot for each group. *C*, the protein–protein interaction network for the 27 proteins that were estimated to have a fold change larger than 2. Each color represents a previous study that suggested these proteins to be involved in osteoarthritis. OA, osteoarthritis.

tissues and subsequent proteolytic activation of lysyl oxidase for the crosslinking of the ECM. POSTN positively regulates osteoblast differentiation (55). It binds tightly to fibronectin and TENA for enhancement of crosslinking of type 1 collagen (54). In this study, this protein was increased in both early- and the late-stage OA in comparison to controls, and there was a 3-fold difference in its levels when comparing early- and late-stage OA. Collagen type I (CO1A1) was found to be increased in the synovial fluid in early-stage OA but not in the late-stage. Additionally, both fibronectin and TENA were found to be increased in late-stage OA, and TENA was found to be increased in early-stage OA. This might be an indicator of increased ECM synthesis. Collagen type III (CO3A1) was increased in early OA but decreased in late-stage OA, compared to controls. Collagen III is known to increase during regeneration and wound healing (56, 57), suggesting an attempted regeneration process in early OA. Taken together, the changes in these proteins suggest altered proliferation and development of chondrocytes, as well as widespread changes in the ECM especially in the early stage of OA.

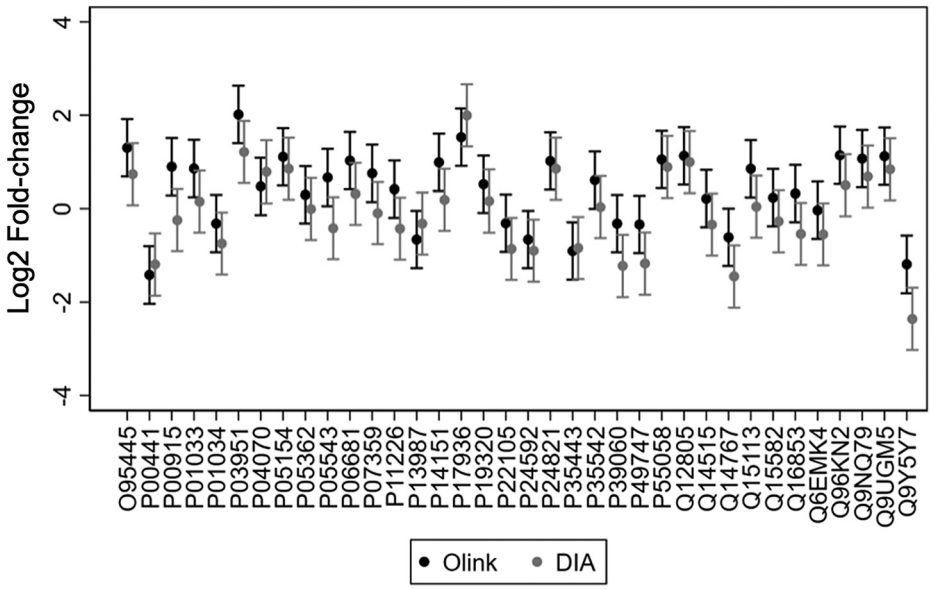

FIG. 5. **Validation of MS data.** Comparison of fold changes for the late-stage OA *versus* controls between the two methods used, DIA and Olink, shown as differences with 95% CIs. DIA, data-independent acquisition; MS, mass spectrometry; OA, osteoarthritis.

Some of the proteins that have a 2-fold or higher change in differential expression in OA patients compared to controls have previously not been reported to be associated with OA disease progression, *e.g.*, ZHX3 and lymphatic vessel endothelial hyaluronic acid receptor 1 (LYVE1). ZHX3 acts as a transcriptional repressor involved in the early stages of mesenchymal stem cell osteogenic differentiation, which plays a fundamental role in skeletal tissue homeostasis (58). It has been suggested to be involved in the switch from the undifferentiated state of MSC to an osteogenic program. The increase of ZHX3 might be an increase of an osteogenic differentiation compensating the catabolic effect detected on the ECM proteins above. LYVE1 is a marker for lymphatic vessels and a decrease of LYVE1 might be an indication of a decreased lymphangiogenesis. It has been reported to plays a role in autocrine regulation of cell growth and as a hyaluronan transporter, either mediating its uptake for catabolism within lymphatic endothelial cells themselves, or its transport into the lumen of afferent lymphatic vessels for subsequent re-uptake and degradation in lymph nodes (59, 60). Decrease in LYVE1 may have a dysregulating effect on the synovial fluid clearance and lymphatic vessel decrease has previously been associated with OA (61). Importantly, lymphatic vessels have only been detected in the synovium but not in the subchondral bone. The differential expression of these proteins that has originate from different compartments of the joint (62), suggests that molecular changes from the whole joint can be detected in synovial fluid. ZHX3 was increased in both early- and late-stage OA while LYVE1 was decreased in the OA patients in comparison to the controls. The positive co-expression of these two proteins seen in controls and in early-stage OA, compared to the rest of the 27 differentially expressed proteins, seemed to be diminished in late-stage OA, suggesting that the cross talk between these proteins is lost. These data could reflect a dysfunction in skeletal tissue homeostasis in late-stage OA.

Among the proteins that were found to be exclusively upregulated in late-stage OA was CRTAC1, a glycosylated ECM protein that can be found in the deep zone of articular cartilage (63, 64). This protein is used as a marker to distinguish chondrocytes from osteoblasts and mesenchymal stem cells in culture. It can be detected in cartilage, bone, and cultured chondrocytes, but not in osteoblasts. The altered expression of this protein in the synovial fluid samples from late-stage OA cases might reflect a severely damaged knee (65). It could also reflect higher exposure of the synovial fluid to the deep zone of articular cartilage.

The transcription factors that were mapped through the differentially expressed proteins to be inhibited in the different OA stages were PPARG and RETN. PPARG has a central role in the regulation of glucose and lipid homeostasis (66–68). The protein network (Fig. 3) suggests PPARG involvement through IGF and insulin-like growth factor binding proteins among others. IGF has previously been shown to play an important role in regulation of glucose uptake by chondrocytes, toward maintenance of intracellular homeostasis (9). Any dysfunction in this endocrine regulation might trigger a metabolic disorder in chondrocyte progression and proliferation. Changes in IGF-I distribution levels and its clearance will have significant effects on cartilage turnover. This suggests an alteration in the metabolic regulation in early-stage OA. RETN is a hormone that suppresses insulin's ability to stimulate glucose uptake into adipose cells, but in synovial fluid from OA patients, it has been associated with an increased catabolic activity and the

initiation of an inflammatory response (69). RETN inhibition in late-stage OA indicates a change in the catabolic activity.

The degree to which inflammation contributes to OA pathogenesis and progression is an ongoing discussion in the field (10, 11, 70–74). There is still controversy whether it is predominantly an inflammatory, a low-grade inflammatory, or a primarily a biomechanically driven disease with secondary inflammation (10, 11, 75). In this study, we have utilized discovery-based MS, which is capable of capturing a high dynamic range of molecules in a sample (76), and we could not find strong evidence of a typical acute phase inflammatory response (77) associated with OA. No change was detected between OA samples and controls regarding complementary factors, alpha-2-macroglobulins, alpha-1-antitrypsin, or serum amyloid A. Cytokines and chemokines were sparsely detected in this dataset, and the differential expression among disease stages of such molecules did not indicate inflammation as the driving force. On the other hand, this analysis may not detect the very low abundant inflammatory markers if no extensive fractionation is carried out. Previous studies supporting inflammation as a driving force of OA were not discovery based and only explored specific inflammatory molecules in biofluids such as blood or plasma (10). The lack of a robust inflammatory signature in our findings matches previous reports using discovery-based proteomics (22, 24–26). On the other hand, the ingenuity pathway analysis suggested IL17 activation in early OA but CXCL12 inhibition in late stage. This could mean that inflammation is a contributor in the early stages in OA but is inhibited in the end. Furthermore, clinical trials that target inflammation, such as IL antagonist therapies and anti-cytokine therapeutic drugs, have failed to reverse OA (78), but the majority of these trials have been conducted with subcutaneous injections rather than intra-articular injections. Although inflammatory molecules could be detected even at a low level, the degree of which they contribute to disease progression remains unknown.

Overall, these results show that a higher proportion of the detected proteins were upregulated in early-stage OA, while late-stage OA was characterized by an imbalance of the homeostasis of the synovial fluid proteome. Furthermore, our data indicate that profiling the proteomic signature of a disease state may not be solely sufficient to elucidate the underlying mechanisms of OA. However, the disrupted cross talk between proteins across different stages of the disease might provide insights into the mechanisms of disease onset and progression.

We would like to acknowledge some important limitations of this study. Four out of seven synovial fluid samples in the early-stage OA group were diluted during aspiration. To compensate for this, their total protein contents were normalized, leaving us with reduced individual variation detected in the differential expression analysis. On the other hand, the co-expression data were based on pairwise comparisons between proteins within the same sample, which is a major strength in this study. This minimizes any type of variation that could have come from the sample preparation or analysis. For the early-stage OA group, the same pattern of an overall increase in protein expression was detected in both the differential expression analysis and the co-expression analysis.

The samples used as controls was from postmortem donors. To our knowledge, there is no study of how quickly death effects the proteome in synovial fluid. Forensic studies have investigated the change of specific biochemical like potassium, glucose, and creatinine (79). Even though only very few metabolites showed a correlation between the concentration and time postmortem, the countable difference was only detected after 120 h (79, 80). In this study, all samples were obtained within 48 h postmortem, and the specimens were frozen at −80 °C within 2 h of extraction to be eligible as controls. Therefore, the proteomic status was assumed to be stable postmortem.

Two hundred forty-one proteins were not included in the statistical analysis due to too large proportion of missing data. Any data imputation was outside the scope of the current work as we suspected data missing not at random. We could detect an increase of hemoglobin subunit alpha in late OA but not in the early OA. We cannot fully exclude nonvisible blood contamination during aspiration of synovial fluid to have affected the increased hemoglobin abundance in late-stage OA. But since the same technique was used in both the early and late OA group when aspirating the synovial fluid, we think that collection procedure is less likely to be the cause of this difference.

CONCLUSIONS

We found profound differences in the protein profiles of synovial fluid from controls and patients with different stages of OA. The synovial fluid of early-stage OA might represent a “raging battlefield” of increased protein activity, while late-stage OA displays the “aftermath”. Further efforts should be made to elucidate the early processes in the disease, which have the greatest potential to be modified by therapeutic interventions.

DATA AVAILABILITY

The mass spectrometry proteomics data have been deposited to the ProteomeXchange Consortium *via* the PRIDE partner repository with the dataset identifier PXD023708.

Supplemental data—This article contains supplemental data.

Acknowledgments—We would also like to thank Hani Alsafadi for the proofreading and the help with the graphical abstract.

Funding and additional information—This work was supported by the European Research Council (ERC) under the European Union's Horizon 2020 research and innovation programme (grant agreement #771121), the Swedish Research Council, the Foundation for Research in Rheumatology (FOREUM), the IAB Lundberg Foundation, the Greta and Johan Kock Foundation, the Swedish Rheumatism Association, the Österlund Foundation, the Governmental Funding of Clinical Research program within the National Health Service (ALF), and the Royal Physiographic Society of Lund and the Faculty of Medicine, Lund University, Sweden. The funders had no role in study design, data collection and analysis, decision to publish, or preparation of the manuscript.

Author contributions—N. A., P. Ö., and M. E. conceptualization; N. A., A. T., P. Ö., and M. E. methodology; N. A. and A. T. software; N. A. and A. T. validation; N. A. and A. T. formal analysis; N. A. investigation; N. A. writing-original draft; N. A., A. T., V. H., E. F., J. T., P. N., P. Ö., and M. E. writing-review and editing; N. A. visualization; A. T., P. Ö., and M. E. supervision; V. H., E. F., P. N., and J. T. resources; V. H. data curation; V. H. project administration; M. E. funding acquisition.

Conflict of interest—The authors declare no competing financial interests.

Abbreviations—The abbreviations used are: ACN, acetonitrile; AGC, automatic gain control; DIA, data-independent acquisition; FA, formic acid; IL, interleukin; LYVE1, lymphatic vessel endothelial hyaluronic acid receptor 1; MS, mass spectrometry; OA, osteoarthritis; PCA, principal component analysis; PPARG, peroxisome proliferator–activated receptor gamma; RETN, resistin.

Received January 28, 2021, and in revised from, November 4, 2021
Published, MCPRO Papers in Press, January 21, 2022, https://doi.org/10.1016/j.mcpro.2022.100200

REFERENCES

1. Wittenauer, R., Smith, L., and Aden, K. (2013) *Background Paper 6.12 Osteoarthritis*. World Health Organisation, Geneva
2. Loeser, R. F., Goldring, S. R., Scanzello, C. R., and Goldring, M. B. (2012) Osteoarthritis: A disease of the joint as an organ. *Arthritis Rheum.* **64**, 1697–1707
3. Loeser, R. F. (2017) The role of aging in the development of osteoarthritis. *Trans. Am. Clin. Climatol. Assoc.* **128**, 44
4. Shane Anderson, A., and Loeser, R. F. (2010) Why is osteoarthritis an age-related disease? *Best Pract. Res. Clin. Rheumatol.* **24**, 15–26
5. Heinegård, D., and Saxne, T. (2011) The role of the cartilage matrix in osteoarthritis. *Nat. Rev. Rheumatol.* **7**, 50–56
6. Zheng, L., Zhang, Z., Sheng, P., and Mobasheri, A. (2021) The role of metabolism in chondrocyte dysfunction and the progression of osteoarthritis. *Ageing Res. Rev.* **66**, 101249
7. Dieppe, P. A., and Lohmander, L. S. (2005) Pathogenesis and management of pain in osteoarthritis. *Lancet* **365**, 965–973
8. Mobasheri, A., Rayman, M. P., Gualillo, O., Sellam, J., van der Kraan, P., and Fearon, U. (2017) The role of metabolism in the pathogenesis of osteoarthritis. *Nat. Rev. Rheumatol.* **13**, 302–311
9. Mobasheri, A., Vannucci, S. J., Bondy, C. A., Carter, S. D., Innes, J. F., Arteaga, M. F., Trujillo, E., Ferraz, I., Shakibaei, M., and Martín-Vasallo, P. (2002) Glucose transport and metabolism in chondrocytes: A key to understanding chondrogenesis, skeletal development and cartilage degradation in osteoarthritis. *Histol. Histopathol.* **17**, 1239–1267
10. Chow, Y. Y., and Chin, K. Y. (2020) The role of inflammation in the pathogenesis of osteoarthritis. *Mediators Inflamm.* **2020**, 8293921
11. Robinson, W. H., Lepus, C. M., Wang, Q., Raghu, H., Mao, R., Lindstrom, T. M., and Sokolove, J. (2016) Low-grade inflammation as a key mediator of the pathogenesis of osteoarthritis. *Nat. Rev. Rheumatol.* **12**, 580–592
12. Martel-Pelletier, J., Barr, A. J., Cicuttini, F. M., Conaghan, P. G., Cooper, C., Goldring, M. B., Goldring, S. R., Jones, G., Teichtahl, A. J., and Pelletier, J. P. (2016) Osteoarthritis. *Nat. Rev. Dis. Primers* **2**, 16072
13. Grässel, S., and Muschter, D. (2020) Recent advances in the treatment of osteoarthritis. *F1000Res.* **9**. F1000 Faculty Rev-325
14. Braun, H. J., and Gold, G. E. (2012) Diagnosis of osteoarthritis: Imaging. *Bone* **51**, 278–288
15. Hunter, D. J., Nevitt, M., Losina, E., and Kraus, V. (2014) Biomarkers for osteoarthritis: Current position and steps towards further validation. *Best Pract. Res. Clin. Rheumatol.* **28**, 61–71
16. Attur, M., Krasnokutsky-Samuels, S., Samuels, J., and Abramson, S. B. (2013) Prognostic biomarkers in osteoarthritis. *Curr. Opin. Rheumatol.* **25**, 136–144
17. Watt, F. E. (2018) Osteoarthritis biomarkers: Year in review. *Osteoarthritis Cartilage* **26**, 312–318
18. Mayeux, R. (2004) Biomarkers: Potential uses and limitations. *NeuroRx* **1**, 182–188
19. Ball, J. R., and Micheel, C. M. (2010) *Evaluation of Biomarkers and Surrogate Endpoints in Chronic Disease*. National Academies Press, Washington, DC
20. Sharma, A. R., Jagga, S., Lee, S. S., and Nam, J. S. (2013) Interplay between cartilage and subchondral bone contributing to pathogenesis of osteoarthritis. *Int. J. Mol. Sci.* **14**, 19805–19830
21. Mobasheri, A. (2011) Applications of proteomics to osteoarthritis, a musculoskeletal disease characterized by aging. *Front Physiol.* **2**, 108
22. Balakrishnan, L., Nirujogi, R. S., Ahmad, S., Bhattacharjee, M., Manda, S. S., Renuse, S., Kelkar, D. S., Subbannayya, Y., Raju, R., Goel, R., Thomas, J. K., Kaur, N., Dhillon, M., Tankala, S. G., Jois, R., *et al*. (2014) Proteomic analysis of human osteoarthritis synovial fluid. *Clin. Proteomics* **11**, 6
23. Peffers, M. J., Smagul, A., and Anderson, J. R. (2019) Proteomic analysis of synovial fluid: Current and potential uses to improve clinical outcomes. *Expert Rev. Proteomics* **16**, 287–302
24. Liao, W., Li, Z., Li, T., Zhang, Q., Zhang, H., and Wang, X. (2018) Proteomic analysis of synovial fluid in osteoarthritis using SWATH-mass spectrometry. *Mol. Med. Rep.* **17**, 2827–2836
25. Brophy, R. H., Cai, L., Duan, X., Zhang, Q., Townsend, R. R., Nunley, R. M., Guilak, F., and Rai, M. F. (2019) Proteomic analysis of synovial fluid identifies periostin as a biomarker for anterior cruciate ligament injury. *Osteoarthritis Cartilage* **27**, 1778–1789
26. Ritter, S. Y., Subbaiah, R., Bebek, G., Crish, J., Scanzello, C. R., Krastins, B., Sarracino, D., Lopez, M. F., Crow, M. K., Aigner, T., Goldring, M. B., Goldring, S. R., Lee, D. M., Gobezie, R., and Aliprantis, A. O. (2013) Proteomic analysis of synovial fluid from the osteoarthritic knee: Comparison with transcriptome analyses of joint tissues. *Arthritis Rheum.* **65**, 981–992
27. Ruiz-Romero, C., Rego-Perez, I., and Blanco, F. J. (2018) What did we learn from 'omics' studies in osteoarthritis. *Curr. Opin. Rheumatol.* **30**, 114–120
28. Tsezou, A. (2014) Osteoarthritis year in review 2014: Genetics and genomics. *Osteoarthritis Cartilage* **22**, 2017–2024
29. Ji, H., and Liu, X. S. (2010) Analyzing 'omics data using hierarchical models. *Nat. Biotechnol.* **28**, 337–340
30. Bland, J. M., and Altman, D. G. (1986) Statistical methods for assessing agreement between two methods of clinical measurement. *Lancet* **1**, 307–310
31. Giavarina, D. (2015) Understanding Bland Altman analysis. *Biochem. Med. (Zagreb)* **25**, 141–151
32. Parente, A., and Sutherland, J. C. (2013) Principal component analysis of turbulent combustion data: Data pre-processing and manifold sensitivity. *Combust. Flame* **160**, 340–350
33. Jolliffe, I. T., and Cadima, J. (2016) Principal component analysis: A review and recent developments. *Philos. Trans. A Math. Phys. Eng. Sci.* **374**, 20150202

34. Zhang, Y., and Pan, W. (2015) Principal component regression and linear mixed model in association analysis of structured samples: Competitors or complements? *Genet. Epidemiol.* **39**, 149–155
35. Ramos, Y. F., den Hollander, W., Bovée, J. V., Bomer, N., van der Breggen, R., Lakenberg, N., Keurentjes, J. C., Goeman, J. J., Slagboom, P. E., Nelissen, R. G., Bos, S. D., and Meulenbelt, I. (2014) Genes involved in the osteoarthritis process identified through genome wide expression analysis in articular cartilage; the RAAK study. *PLoS One* **9**, e103056
36. Fernandes, A. M., Herlofsen, S. R., Karlsen, T. A., Küchler, A. M., Fløisand, Y., and Brinchmann, J. E. (2013) Similar properties of chondrocytes from osteoarthritis joints and mesenchymal stem cells from healthy donors for tissue engineering of articular cartilage. *PLoS One* **8**, e62994
37. Ryd, L., Brittberg, M., Eriksson, K., Jurvelin, J. S., Lindahl, A., Marlovits, S., Möller, P., Richardson, J. B., Steinwachs, M., and Zenobi-Wong, M. (2015) Pre-osteoarthritis: Definition and diagnosis of an elusive clinical entity. *Cartilage* **6**, 156–165
38. Hulme, C. H., Wilson, E. L., Peffers, M. J., Roberts, S., Simpson, D. M., Richardson, J. B., Gallacher, P., and Wright, K. T. (2017) Autologous chondrocyte implantation-derived synovial fluids display distinct responder and non-responder proteomic profiles. *Arthritis Res. Ther.* **19**, 150
39. Grogan, S. P., Chen, X., Sovani, S., Taniguchi, N., Colwell, C. W., Lotz, M. K., and D'Lima, D. D. (2014) Influence of cartilage extracellular matrix molecules on cell phenotype and neocartilage formation. *Tissue Eng. Part A* **20**, 264–274
40. Gobezie, R., Kho, A., Krastins, B., Sarracino, D. A., Thornhill, T. S., Chase, M., Millett, P. J., and Lee, D. M. (2007) High abundance synovial fluid proteome: Distinct profiles in health and osteoarthritis. *Arthritis Res. Ther.* **9**, R36
41. Taipale, M., Solovieva, S., Leino-Arjas, P., and Männikkö, M. (2017) Functional polymorphisms in asporin and CILP together with joint loading predispose to hand osteoarthritis. *BMC Genet.* **18**, 108
42. Fernández-Puente, P., González-Rodríguez, L., Calamia, V., Picchi, F., Lourido, L., Camacho-Encina, M., Oreiro, N., Rocha, B., Paz-González, R., Marina, A., García, C., Blanco, F. J., and Ruiz-Romero, C. (2019) Analysis of endogenous peptides released from osteoarthritic cartilage unravels novel pathogenic markers. *Mol. Cell. Proteomics* **18**, 2018–2028
43. Han, B., Li, Q., Wang, C., Patel, P., Adams, S. M., Doyran, B., Nia, H. T., Oftadeh, R., Zhou, S., Li, C. Y., Liu, X. S., Lu, X. L., Enomoto-Iwamoto, M., Qin, L., Mauck, R. L., *et al*. (2019) Decorin regulates the aggrecan network integrity and biomechanical functions of cartilage extracellular matrix. *ACS Nano* **13**, 11320–11333
44. Johnson, K., Farley, D., Hu, S. I., and Terkeltaub, R. (2003) One of two chondrocyte-expressed isoforms of cartilage intermediate-layer protein functions as an insulin-like growth factor 1 antagonist. *Arthritis Rheum.* **48**, 1302–1314
45. Lorenzo, P., Bayliss, M. T., and Heinegård, D. (2004) Altered patterns and synthesis of extracellular matrix macromolecules in early osteoarthritis. *Matrix Biol.* **23**, 381–391
46. Lorenzo, P., Bayliss, M. T., and Heinegård, D. (1998) A novel cartilage protein (CILP) present in the mid-zone of human articular cartilage increases with age. *J. Biol. Chem.* **273**, 23463–23468
47. Kiani, C., Chen, L., Wu, Y. J., Yee, A. J., and Yang, B. B. (2002) Structure and function of aggrecan. *Cell Res.* **12**, 19–32
48. Roughley, P. J., and Mort, J. S. (2014) The role of aggrecan in normal and osteoarthritic cartilage. *J. Exp. Orthop.* **1**, 8
49. Chandran, P. L., and Horkay, F. (2012) Aggrecan, an unusual polyelectrolyte: Review of solution behavior and physiological implications. *Acta Biomater.* **8**, 3–12
50. Heinegård, D., and Hascall, V. C. (1974) Aggregation of cartilage proteoglycans. 3. Characteristics of the proteins isolated from trypsin digests of aggregates. *J. Biol. Chem.* **249**, 4250–4256
51. Sandy, J. D., and Verscharen, C. (2001) Analysis of aggrecan in human knee cartilage and synovial fluid indicates that aggrecanase (ADAMTS) activity is responsible for the catabolic turnover and loss of whole aggrecan whereas other protease activity is required for C-terminal processing *in vivo*. *Biochem. J.* **358**, 615–626
52. Ni, G. X., Li, Z., and Zhou, Y. Z. (2014) The role of small leucine-rich proteoglycans in osteoarthritis pathogenesis. *Osteoarthritis Cartilage* **22**, 896–903
53. Heinegård, D. (2009) Fell-Muir Lecture: Proteoglycans and more–from molecules to biology. *Int. J. Exp. Pathol.* **90**, 575–586
54. Kudo, A. (2017) Introductory review: Periostin—gene and protein structure. *Cell. Mol. Life Sci.* **74**, 4259–4268
55. Oshima, A., Tanabe, H., Yan, T., Lowe, G. N., Glackin, C. A., and Kudo, A. (2002) A novel mechanism for the regulation of osteoblast differentiation: Transcription of periostin, a member of the fasciclin I family, is regulated by the bHLH transcription factor, twist. *J. Cell Biochem.* **86**, 792–804
56. Xue, M., and Jackson, C. J. (2015) Extracellular matrix reorganization during wound healing and its impact on abnormal scarring. *Adv. Wound Care* **4**, 119–136
57. Hsueh, M. F., Kraus, V. B., and Önnerfjord, P. (2017) Cartilage matrix remodelling differs by disease state and joint type. *Eur. Cell Mater.* **34**, 70–82
58. Suehiro, F., Nishimura, M., Kawamoto, T., Kanawa, M., Yoshizawa, Y., Murata, H., and Kato, Y. (2011) Impact of zinc fingers and homeoboxes 3 on the regulation of mesenchymal stem cell osteogenic differentiation. *Stem Cells Dev.* **20**, 1539–1547
59. Banerji, S., Ni, J., Wang, S. X., Clasper, S., Su, J., Tammi, R., Jones, M., and Jackson, D. G. (1999) LYVE-1, a new homologue of the CD44 glycoprotein, is a lymph-specific receptor for hyaluronan. *J. Cell Biol.* **144**, 789–801
60. Lawrance, W., Banerji, S., Day, A. J., Bhattacharjee, S., and Jackson, D. G. (2016) Binding of hyaluronan to the native lymphatic vessel endothelial receptor LYVE-1 is critically dependent on receptor clustering and hyaluronan organization. *J. Biol. Chem.* **291**, 8014–8030
61. Walsh, D. A., Verghese, P., Cook, G. J., McWilliams, D. F., Mapp, P. I., Ashraf, S., and Wilson, D. (2012) Lymphatic vessels in osteoarthritic human knees. *Osteoarthritis Cartilage* **20**, 405–412
62. Timur, U. T., Jahr, H., Anderson, J., Green, D. C., Emans, P. J., Smagul, A., van Rhijn, L. W., Peffers, M. J., and Welting, T. J. M. (2021) Identification of tissue-dependent proteins in knee OA synovial fluid. *Osteoarthritis Cartilage* **29**, 124–133
63. Steck, E., Benz, K., Lorenz, H., Loew, M., Gress, T., and Richter, W. (2001) Chondrocyte expressed protein-68 (CEP-68), a novel human marker gene for cultured chondrocytes. *Biochem. J.* **353**, 169–174
64. Steck, E., Bräun, J., Pelttari, K., Kadel, S., Kalbacher, H., and Richter, W. (2007) Chondrocyte secreted CRTAC1: A glycosylated extracellular matrix molecule of human articular cartilage. *Matrix Biol.* **26**, 30–41
65. Styrkarsdottir, U., Lund, S. H., Saevarsdottir, S., Magnusson, M. I., Gunnarsdottir, K., Norddahl, G. L., Frigge, M. L., Ivarsdottir, E. V., Bjornsdottir, G., Holm, H., Thorgeirsson, G., Rafnar, T., Jonsdottir, I., Ingvarsson, T., Jonsson, H., *et al*. (2021) The CRTAC1 protein in plasma is associated with osteoarthritis and predicts progression to joint replacement: A large-scale proteomics scan in Iceland. *Arthritis Rheumatol.* **73**, 2025–2034
66. Stanton, L. A., Li, J. R., and Beier, F. (2010) PPARgamma2 expression in growth plate chondrocytes is regulated by p38 and GSK-3. *J. Cell. Mol. Med.* **14**, 242–256
67. Kim, D. H., Kim, D. H., Heck, B. E., Shaffer, M., Yoo, K. H., and Hur, J. (2020) PPAR-δ agonist affects adipo-chondrogenic differentiation of human mesenchymal stem cells through the expression of PPAR-γ. *Regen. Ther.* **15**, 103–111
68. Huang, G., Jiang, W., Xie, W., Lu, W., Zhu, W., and Deng, Z. (2021) Role of peroxisome proliferator-activated receptors in osteoarthritis (review). *Mol. Med. Rep.* **23**, 159
69. Koskinen, A., Vuolteenaho, K., Moilanen, T., and Moilanen, E. (2014) Resistin as a factor in osteoarthritis: Synovial fluid resistin concentrations correlate positively with interleukin 6 and matrix metalloproteinases MMP-1 and MMP-3. *Scand. J. Rheumatol.* **43**, 249–253
70. Hsu, H., and Siwiec, R. M. (2022) Knee osteoarthritis. In: *StatPearls [Internet]*. StatPearls Publishing, Treasure Island, FL
71. van den Bosch, M. H. J. (2019) Inflammation in osteoarthritis: Is it time to dampen the alarm(in) in this debilitating disease? *Clin. Exp. Immunol.* **195**, 153–166
72. Berenbaum, F., and Walker, C. (2020) Osteoarthritis and inflammation: A serious disease with overlapping phenotypic patterns. *Postgrad. Med.* **132**, 377–384

73. Loureiro, A., Mills, P. M., and Barrett, R. S. (2013) Muscle weakness in hip osteoarthritis: A systematic review. *Arthritis Care Res. (Hoboken)* **65**, 340–352
74. Roos, E. M., Herzog, W., Block, J. A., and Bennell, K. L. (2011) Muscle weakness, afferent sensory dysfunction and exercise in knee osteoarthritis. *Nat. Rev. Rheumatol.* **7**, 57–63
75. de Lange-Brokaar, B. J., Ioan-Facsinay, A., van Osch, G. J., Zuurmond, A. M., Schoones, J., Toes, R. E., Huizinga, T. W., and Kloppenburg, M. (2012) Synovial inflammation, immune cells and their cytokines in osteoarthritis: A review. *Osteoarthritis Cartilage* **20**, 1484–1499
76. Petrera, A., von Toerne, C., Behler, J., Huth, C., Thorand, B., Hilgendorff, A., and Hauck, S. M. (2021) Multiplatform approach for plasma proteomics: Complementarity of Olink proximity extension assay technology to mass spectrometry-based protein profiling. *J. Proteome Res.* **20**, 751–762
77. Gruys, E., Toussaint, M. J., Niewold, T. A., and Koopmans, S. J. (2005) Acute phase reaction and acute phase proteins. *J. Zhejiang Univ. Sci. B* **6**, 1045–1056
78. Haseeb, A., and Haqqi, T. M. (2013) Immunopathogenesis of osteoarthritis. *Clin. Immunol.* **146**, 185–196
79. Madea, B., Kreuser, C., and Banaschak, S. (2001) Postmortem biochemical examination of synovial fluid–a preliminary study. *Forensic Sci. Int.* **118**, 29–35
80. Holley, H. L., Patton, F. M., Pigman, W., and Platt, D. (1956) An electrophoretic study of normal and post-mortem human and bovine synovial fluids. *Arch. Biochem. Biophys.* **64**, 152–163